Multi-Level PET and CT Fusion Radiomics-based Survival Analysis of NSCLC Patients

Mehdi Amini, Mostafa Nazari, Isaac Shiri, Ghasem Hajianfar, Mohammad Reza Deevband, Hamid Abdollahi and Habib Zaidi, *Fellow, IEEE*

2020 IEEE Nuclear Science Symposium and Medical Imaging Conference (NSS/MIC) | 978-1-7281-7693-2/20/$31.00 ©2020 IEEE | DOI: 10.1109/NSS/MIC42677.2020.9507759

***Abstract*– To provide a comprehensive characterization of intra-tumor heterogeneity, this study proposes multi-level multi-modality radiomic models derived from ^{18}F-FDG PET and CT images by feature- and image-level fusion. Specifically, we developed fusion radiomic models to improve overall survival prediction of NSCLC patients. In this work, a NSCLC dataset including patients from two different institutions (86 patients used as training and 95 patients used as testing) was included. By extracting 225 features from CT, PET, and fused images, radiomics analysis was used to build single-modality and multi-modality models where the fused images are constructed by 3D-wavelet transform fusion (WF). Two models were also developed using two feature-level fusion strategies of feature concatenation (ConFea) and feature averaging (AvgFea). Cox proportional hazard (Cox PH) regression was utilized for survival analysis. Spearman's correlation was utilized as a measure of redundancy, and then best combination of 10 most related features (ranked by univariate Cox PH) were fed into multivariate Cox model. Moreover, the median prognostic score captured from training cohort was used as an untouched threshold in the test cohort to stratify patients into low- and high-risk groups. The difference between groups was assessed using log-rank test. Among all models, WF (C-index=0.708) had the highest index and significantly outperformed CT and PET (C-index = 0.616, 0.572, respectively). Image-level fusion model also outperformed feature-level fusion models ConFea and AvgFea (C-indices = 0.581, 0.641, respectively). Our results demonstrate that multi-modal radiomics models especially models fused at image-level have the potential to improve prognosis by combining information from different tumor characteristics, including anatomical and metabolic captured by different imaging modalities.**

***Index Terms*—PET, CT, Radiomics, NSCLC**

Manuscript was submitted Dec 20, 2020. This work was supported by the Swiss National Science Foundation under grant SNSF 320030_176052 and Shahid Beheshti University of Medical Sciences.

M. Amini, M. Nazari, and MR Deevband are with the Department of Biomedical Engineering and Medical Physics, Shahid Beheshti University of Medical Sciences, Tehran, Iran. (e-mail: mehdi.amini.1994.ma@gmail.com, msnaa1392@gmail.com, mdeevband@sbmu.ac.ir)

I. Shiri, and H. Zaidi, are with Division of Nuclear Medicine and Molecular Imaging, Geneva University Hospital, Geneva, Switzerland (e-mail: Isaac.shirilord@unige.ch, habib.zaidi@hcuge.ch).

G. Hajianfar is with Rajaie Cardiovascular Medical and Research Center, Iran University of Medical Science, Tehran, Iran (e-mail: hajianfar.gh@gmail.com)

H. Abdolahi. is with Department of Radiologic Sciences and Medical Physics, Kerman University of Medical Science, Kerman, Iran (e-mail: hamid_rbp@yahoo.com)

H. Zaidi is with Geneva University Neurocenter, Geneva University, Geneva, Switzerland.

I. Introduction

The lungs are among the most common hosts of cancer, which is also the leading cause of cancer deaths [1]. About 85% of lung cancers are non-small cell lung carcinomas (NSCLC) [1]. Accurate classification of non-small cell lung cancer (NSCLC) patients into groups is vital to optimize treatment strategies. This stratification establishes treatment plans that best fit each individual's condition. Currently tumor Node Metastasis (TNM) staging system is an accepted clinical framework which is used to classify patients into stages [2]. However, it's intrinsic limitations makes it an indelicate procedure which results in wide range of survivals for patients with same stages [3]. Besides TNM, Omics approaches (proteomics, and genomics) can provide a potential to improve prognosis by decoding intra-tumor heterogeneity (ITH) in lung cancer patients [4-6]. However, it's not possible to provide a complete characterization of tumor heterogeneity with these methods regarding their invasive procedure and limited samplings [7, 8]. New insights in ITH along with advancements in the emerging field of radiomics is promising to decode ITH characteristics and develop precise cancer prognostic models [9-12]. Radiomics analysis of tumors has been widely investigated on single imaging modalities, such as ^{18}F-FDG PET [13] and CT scans [7, 14]. However, each modality demonstrates different characteristics of tumor heterogeneity. Integration of information from different modalities for radiomics analysis can be accomplished for different levels of fusion (e.g. feature and image level fusion). Primary studies investigated the potential added prognostic value by concatenating features (feature-level fusion) from different imaging modalities [15, 16]. Other studies such as [17] utilized image-level fusion, and most recently [18] characterized intra-tumor heterogeneity in head and neck cancer, through a multi-level multi-modality strategy, by fusing PET and CT information at image-, matrix- and feature-levels. To the best of our knowledge, there this is the first study investigating and comparing the prognostic value of multi-modality multi-level fusion radiomics models in an all-inclusive manner for NSCLC patients. In the current work, our main attempt was reflecting a comprehensive view of NSCLC tissue characteristics by integrating information mined from PET and CT scans. Toward this goal, we first integrated PET and CT information via image- and feature-level fusion strategies to develop multimodality Radiomics models and

978-1-7281-7693-2/20/$31.00 ©2020 IEEE

then assessed the potential of these models in providing a better overall survival prognosis in NSCLC patients.

II. MATERIALS AND METHODS

A. PET/CT datasets

This study was retrospectively conducted on a PET/CT dataset of NSCLC from The Cancer Imaging Archive (TCIA) [19]. Dataset comprised 211 histologically proven NCSLC patients from two independent institutions. Some patients were excluded from the study owing to technical problems, such as noise, artifacts and image registration issues. Overall, 182 patients (87 from center#1 used as training and 95 from center#2 used as testing cohorts) were included in the current study.

B. Feature extraction framework

In feature extraction first, all lesions identified on PET and CT images were delineated and segmented manually using OSIRIX® and 3D-slicer and then merged into a single mask. Single-modality PET and CT models were constructed. Then PET and CT information were integrated using image- and feature-level fusions to construct multi-modality models. In feature-level fusion, features were extracted from separate scans and then two different approaches of feature concatenation (ConFea) and feature averaging (AvgFea) were pursued. In image-level fusion, features were extracted from a single image, obtained by fused PET and CT scans. We adopted a wavelet-based technique based on 3D discrete wavelet transform (DWT) to combine the spatial and frequency characteristics of CT and PET imaging modalities. Prior to the wavelet fusion (WF) both scans were resampled to equal resolution with isotropic voxel spacing of $2\times2\times2$ mm^3. First, wavelet basis function symlet8 was used to decompose scans were to one decomposition level, and then in order to obtain a single set of fused wavelet coefficients, spatially corresponding wavelet coefficients were weight-averaged. Finally, the fused image was reconstructed by applying the 3D inverse DWT to the set of fused wavelet coefficients.

Overall, 225 radiomics features (79 first-order features such as morphological, statistical, and histogram and features, 136 three-dimensional textural features from GLCM, GLRLM, GLSZM, GLDZM, NGTDM, NGLDM, and 10 moment invariant features) were extracted from scans. Feature extraction was performed using the Standardized Environment for Radiomics Analysis (SERA) Package [20], which obeys guidelines from the Image Biomarker Standardization Initiative (IBSI).

C. Statistical framework

As an endpoint, overall survival (OS) was considered. First, we apply Spearman's correlation coefficient as a measure of redundancy. Then, feature-set reduction was conducted for each of the initial feature-sets via univariate Cox analysis by performing 100 repetitions in the training cohort and the prognostic performance of each feature was measured using concordance index (C-index) and ten top relevant features with the highest C-indices were selected for each model to use in further multivariate analysis. For each of the reduced feature sets, all possible combinations of features were constructed and fitted on training set to identify optimal combination of features. For the assessment of the model performance, Harrell's C-index was measured with 1000 times bootstrap. Eventually, in order to have a dichotomization perspective of our models, we constructed a prognostic score for each patient by taking the linear predictor (i.e. weighted sum of the features in the model, where the weights are the Cox regression coefficients) from the Cox model and then used it's median achieved from training cohorts, untouched, as a threshold to classify patients into low- and high-risk groups in the test cohort. Then groups were projected to Kaplan Meier curves and log rank test was applied to find the difference between subsets. P-values lower than 0.05 were considered significant. All statistical analyses were performed using R package.

III. RESULTS

All reported results are related to the testing cohort. The mean and standard deviation (SD) of C-indices and P-values for each model are listed in Table 1. Fig. 1 presents the Kaplan-Meier curves of single-modalities, feature-level fusion models, and wavelet fusion model. While None of single-modality models and feature-level fusion models reached C-index higher than 0.7, image-level fusion model reached higher C-index of 0.708. Regarding continuous time to event analysis task, highest performance was achieved by WF (C-index: 0.708). And in case of outcome dichotomization (classification) AvgFea reached best performance with p-value of 0.025.

TABLE I. C-INDEX AND P-VALUES FOR THE DIFFERENT MODELS.

Model	C-index	P-value
CT	0.616	0.086
PET	0.572	0.053
AvgFea	0.641	0.025
ConFea	0.581	0.036
WF	0.708	0.027

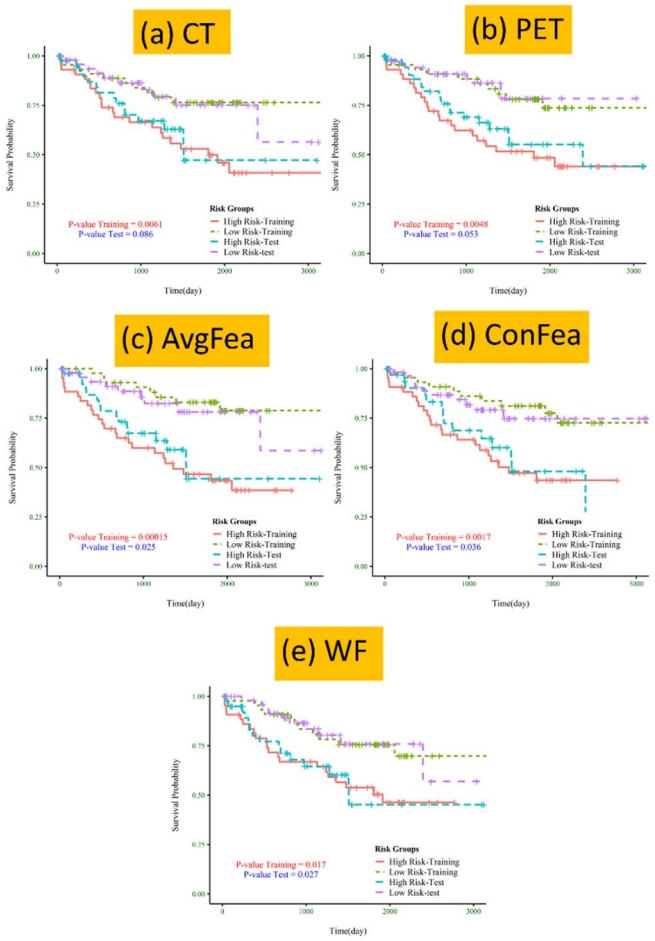

Fig. 1. Kaplan-Meier curves of (a, b) single-modalities, (c, d) feature-level fusion models, (e) image-level wavelet fusion model. The curves for training and testing cohorts are color coded as shown in the legend. P-values are shown for both training and testing datasets.

The performance of all models was compared by applying student's t-test on resulting C-indices and p-values lower than 0.05 were considered significant. Fig. 2 shows the results of comparison. Feature-level fusion model AvgFea was able to outperform both PET and CT models, but ConFea only outperformed PET while was dominated by CT. Image-level fusion model WF significantly outperformed not only PET

SD	C-index					
0.048	0.641	AvgFea	<0.001	<0.001	_	<0.001
0.050	0.581	ConFea	<0.001	<0.001	<0.001	_
0.051	0.707	WF	<0.001	<0.001	<0.001	<0.001
			CT	PET	AvgFea	ConFea
		C-index	0.616	0.572	0.641	0.581
		SD	0.057	0.055	0.480	0.050

Fig. 2. Comparison of models performance via student's t-test. P-values are shown. P-values in which a fusion model outperforms single-modality model are shown in blue, and red for vice versa.

and CT models (C-indices = 0.572 and 0.616, respectively) but also the AvgFea and ConFea (C-indices = 0.641 and 0.581).

IV. DISCUSSION

In this study, we investigated the prognostic value of multi-modality Radiomics models by combining information obtained from PET and CT scans, at feature and image level, toward survival prediction in NSCLC patients. The center hypothesis of this study was to improve quantification of intra-tumor heterogeneity and subsequently the prediction of overall survival in NSCLC patients by merging the anatomical information obtained from tissue density provided by CT, and the functional data obtained from glucose metabolism reflected by ^{18}FDG-PET. Overall, our results show that, image-level fusion shows superiority in simultaneously capturing the information from two modalities. Thus we can say that, by integrating the information obtained from different imaging modalities at image-level fusion we can achieve prognostic models more accurate than single-modality models.

There were some limitations regarding this study such as The fact that segmentations were performed manually and features reproducibility were ignored, which reduces the reproducibility of the study [21-23]. For further studies we suggest richer datasets, and consideration of various image-level fusion methods. In this study, we offered unprecedented radiomics models, by integrating information of 18F-FDG PET and CT images using feature- and image-level fusion, toward an improved prognosis in NCSLC patients. Overall, our multimodality models showed superiority compared to single-modality models. But their superiority depended on the fusion strategy .

REFERENCES

[1] J. Chen *et al.*, "LINC00173. v1 promotes angiogenesis and progression of lung squamous cell carcinoma by sponging miR-511-5p to regulate VEGFA expression," *Molecular Cancer,* vol. 19, no. 1, pp. 1-19, 2020.

[2] P. Goldstraw *et al.*, "The IASLC lung cancer staging project: proposals for revision of the TNM stage groupings in the forthcoming (eighth) edition of the TNM classification for lung cancer," *Journal of Thoracic Oncology,* vol. 11, no. 1, pp. 39-51, 2016.

[3] K. Chansky, J.-P. Sculier, J. J. Crowley, D. Giroux, J. Van Meerbeeck, and P. Goldstraw, "The International Association for the Study of Lung Cancer Staging Project: prognostic factors and pathologic TNM stage in surgically managed non-small cell lung cancer," *Journal of thoracic oncology,* vol. 4, no. 7, pp. 792-801, 2009.

[4] C. G. A. R. Network, "Comprehensive molecular profiling of lung adenocarcinoma," *Nature,* vol. 511, no. 7511, pp. 543-550, 2014.

[5] N. McGranahan and C. Swanton, "Clonal heterogeneity and tumor evolution: past, present, and the future," *Cell,* vol. 168, no. 4, pp. 613-628, 2017.

[6] Z. Chen, C. M. Fillmore, P. S. Hammerman, C. F. Kim, and K.-K. Wong, "Non-small-cell lung cancers: a heterogeneous set of diseases," *Nature Reviews Cancer,* vol. 14, no. 8, pp. 535-546, 2014.

[7] D. L. Longo, "Tumor heterogeneity and personalized medicine," *N Engl J Med,* vol. 366, no. 10, pp. 956-7, 2012.

[8] M. Nazari *et al.*, "Noninvasive Fuhrman grading of clear cell renal cell carcinoma using computed tomography radiomic features and machine learning," (in eng), *Radiol Med,* vol. 125, no. 8, pp. 754-762, Aug 2020.

[9] M. Scrivener, E. E. de Jong, J. E. van Timmeren, T. Pieters, B. Ghaye, and X. Geets, "Radiomics applied to lung cancer: a review," *Transl Cancer Res,* vol. 5, no. 4, pp. 398-409, 2016.

[10] M. Nazari, I. Shiri, and H. Zaidi, "Radiomics-based machine learning model to predict risk of death within 5-years in clear cell renal cell carcinoma patients," (in eng), *Comput Biol Med,* vol. 129, p. 104135, Nov 23 2020.

[11] S. Mostafaei *et al.*, "CT imaging markers to improve radiation toxicity prediction in prostate cancer radiotherapy by stacking regression algorithm," (in eng), *Radiol Med,* vol. 125, no. 1, pp. 87-97, Jan 2020.

[12] G. Hajianfar *et al.*, "Noninvasive O6 Methylguanine-DNA Methyltransferase Status Prediction in Glioblastoma Multiforme Cancer Using Magnetic Resonance Imaging Radiomics Features: Univariate and Multivariate Radiogenomics Analysis," *World Neurosurgery,* vol. 132, pp. e140-e161, 2019/12/01/ 2019.

[13] F. Tixier *et al.*, "Visual versus quantitative assessment of intratumor 18F-FDG PET uptake heterogeneity: prognostic value in non–small cell lung cancer," *Journal of Nuclear Medicine,* vol. 55, no. 8, pp. 1235-1241, 2014.

[14] X. Wang, H. Duan, X. Li, X. Ye, G. Huang, and S. Nie, "A prognostic analysis method for non-small cell lung cancer based on the computed tomography radiomics," *Physics in Medicine & Biology,* vol. 65, no. 4, p. 045006, 2020.

[15] M. Kirienko *et al.*, "Prediction of disease-free survival by the PET/CT radiomic signature in non-small cell lung cancer patients undergoing surgery," *European journal of nuclear medicine and molecular imaging,* vol. 45, no. 2, pp. 207-217, 2018.

[16] M. Vaidya, K. M. Creach, J. Frye, F. Dehdashti, J. D. Bradley, and I. El Naqa, "Combined PET/CT image characteristics for radiotherapy tumor response in lung cancer," *Radiotherapy and Oncology,* vol. 102, no. 2, pp. 239-245, 2012.

[17] M. Vallières, C. R. Freeman, S. R. Skamene, and I. El Naqa, "A radiomics model from joint FDG-PET and MRI texture features for the prediction of lung metastases in soft-tissue sarcomas of the extremities," *Physics in Medicine & Biology,* vol. 60, no. 14, p. 5471, 2015.

[18] W. Lv, S. Ashrafinia, J. Ma, L. Lu, and A. Rahmim, "Multi-level multi-modality fusion radiomics: application to PET and CT imaging for prognostication of head and neck cancer," *IEEE journal of biomedical and health informatics,* vol. 24, no. 8, pp. 2268-2277, 2019.

[19] S. Bakr *et al.*, "A radiogenomic dataset of non-small cell lung cancer," *Scientific data,* vol. 5, no. 1, pp. 1-9, 2018.

[20] S. Ashrafinia, "Quantitative nuclear medicine imaging using advanced image reconstruction and radiomics," Johns Hopkins University, 2019.

[21] I. Shiri *et al.*, "Repeatability of radiomic features in magnetic resonance imaging of glioblastoma: Test-retest and image registration analyses," (in eng), *Med Phys,* vol. 47, no. 9, pp. 4265-4280, Sep 2020.

[22] M. Edalat-Javid *et al.*, "Cardiac SPECT radiomic features repeatability and reproducibility: A multi-scanner phantom study," (in eng), *J Nucl Cardiol,* Apr 24 2020, doi: 10.1007/s12350-020-02109-0.

[23] H. Abdollahi, I. Shiri, and M. Heydari, "Medical Imaging Technologists in Radiomics Era: An Alice in Wonderland Problem," (in eng), *Iran J Public Health,* vol. 48, no. 1, pp. 184-186, Jan 2019.